Electronic Supporting Information

Design of Fe/Co-N doped porous carbon sheets by hard template strategy as an oxygen reduction catalyst for Mg-air batteries

Kun Liu [a], Yujing Ling [a], Xianglong Guan [a], Ke Hu [a], Angli Zhang [a], Kaiqi Liu [a], Haoyi Li [a], Guangnian Xu[a*], Xucheng Fu [b*]

[a] *Anhui Provincial Laboratory of Biomimetic Sensor and Detecting Technology, College of Materials and Chemical Engineering, West Anhui University, Lu'an 237012, Anhui Province, China.*

[b] *Analytical and Testing Center, West Anhui University, Lu'an 237012, Anhui Province, China*

Electrochemical measurements

The Koutecky-Levich diagrams (J^{-1} vs $\omega^{-1/2}$) were investigated at various electrode potentials. The Koutecky-Levich equation enables the determination of oxygen reduction electron transfer number (n) by calculating the slope of its linear regression line. The kinetic properties of the prepared samples can be assessed using the following Koutecky-Levich equation:[1, 2]

$$\frac{1}{j}=\frac{1}{j_L}+\frac{1}{j_K}=\frac{1}{B\omega^{1/2}}+\frac{1}{j_K} \quad \text{Equation (1)}$$

$$B=0.62nFC_0D_0^{2/3}\upsilon^{-1/6} \quad \text{Equation (2)}$$

For the Tafel plot, the kinetic current was calculated as equation (3):

$$j_K=\frac{j\times j_L}{j_L-j} \quad \text{Equation (3)}$$

The experimentally determined current density, labeled as j, is compared against both the diffusional-limited current density (j_L) and dynamic current density (j_K). The rotational speed of the electrode is denoted as ω in radians per second. F denotes the Faraday constant at a value of 96485 $C\cdot mol^{-1}$. Additionally, C_0 corresponds to the volume concentration of O_2 in 0.1 M KOH at a magnitude

of 1.2×10^{-3} mol·L^{-1}, while D_0 represents its diffusion coefficient at a rate of 1.9×10^{-5} $cm^2\cdot s^{-1}$. Furthermore, ν signifies the kinematic viscosity of the electrolyte with an assigned value equaling 0.01 $cm^2\cdot S^{-1}$.

The rotating ring disk electrode (RRDE) technique was employed to determine the transfer number (n), providing values for both the electron transfer number (n) and hydrogen peroxide yield ($\%H_2O_2$) in the formula as follows:

$$\%HO_2^- = 200\times\frac{I_r/N}{I_d + I_r/N} \quad (4)$$

$$n = 4\times\frac{I_d}{I_d + I_r/N} \quad (5)$$

Where I_d represents disk current, I_r represents ring current, and N represents current collection efficiency of the Pt ring (0.424).

Assembly and performance evaluation of magnesium-air batteries

The traditional assembly method was employed to evaluate the performance of the magnesium air battery, utilizing the air electrode, polished magnesium foil, and 3.5wt % NaCl as the cathode, anode, and electrolyte respectively. Nickel foam with excellent conductivity was utilized as a fluid collector for the air electrode. The air electrode is prepared by blending the aforementioned catalyst, ketjenblack, acetylene black, and polytetrafluoroethylene (PTFE) in a weight ratio of 3:3:1:3. The mixture is then dispersed in ethanol to form a homogeneous slurry. Grind and stir the paste until it reaches a smooth consistency, then roll out the catalytic layer to a thickness of approximately 0.2 mm. Using Hefei Kejing's roller press (MSK-HRp-MR100A), compress the air electrode to a thickness range of 0.3-0.5mm (3cm×5cm). Finally, vacuum dry the air electrode at 60°C for 12 hours. The NEWARE battery test system (CT-4008 T-5V12A) was utilized to assess the discharge performance of the catalyst as the cathode in a magnesium air battery. The evaluation was conducted using a domestic magnesium air battery mold (purchased from Changzhou Keyoute Company, Jiangsu Province). Prior to testing, each magnesium foil underwent meticulous polishing, and subsequently these prepared samples were subjected to current densities of 2.5 mA cm^{-2} for discharge property analysis. The discharge curve of the magnesium air battery was obtained through constant discharge methodology.

Supporting Figures

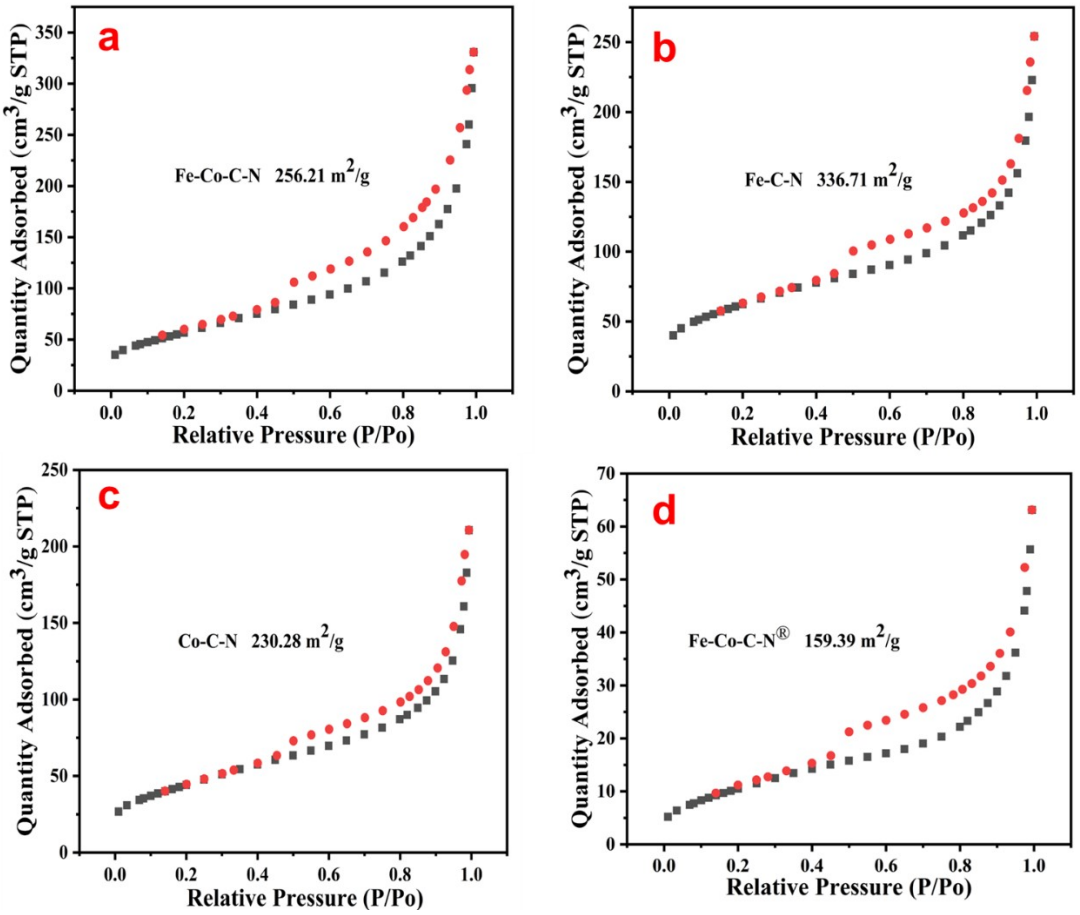

Figure S1. N_2 adsorption-desorption isotherms of (a) Fe-Co-C-N, (b) Fe-C-N, (c)Co-C-N, and (d)Fe-Co-C-N®.

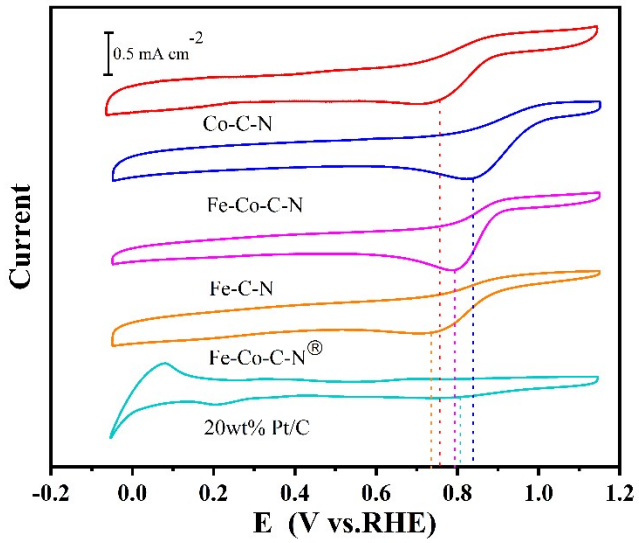

Figure S2. CV curves of different catalyst samples in O_2-saturated electrolyte.

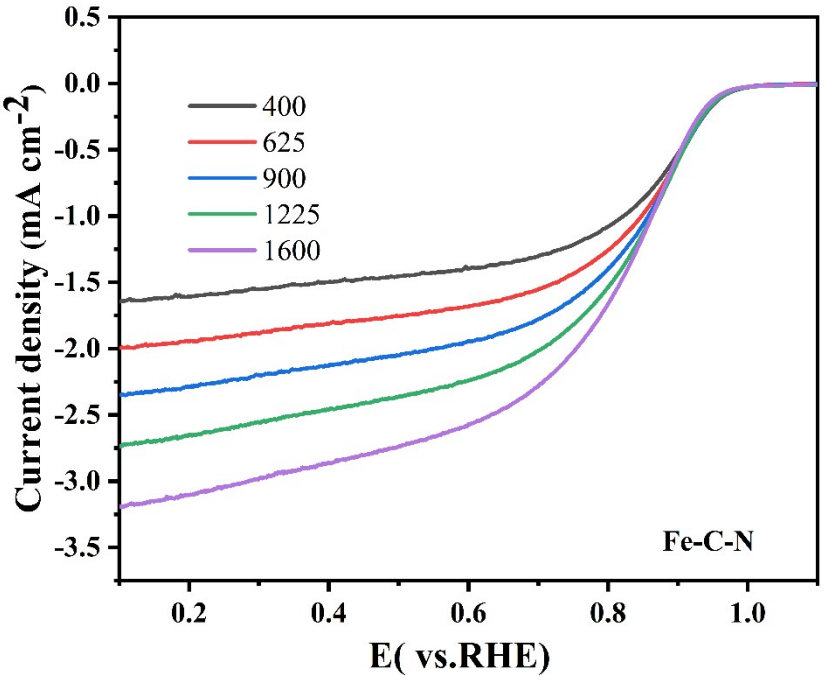

Figure S3. LSV curves of Fe-C-N at different rotation speed (400-1600 rpm) in O_2-saturated electrolyte.

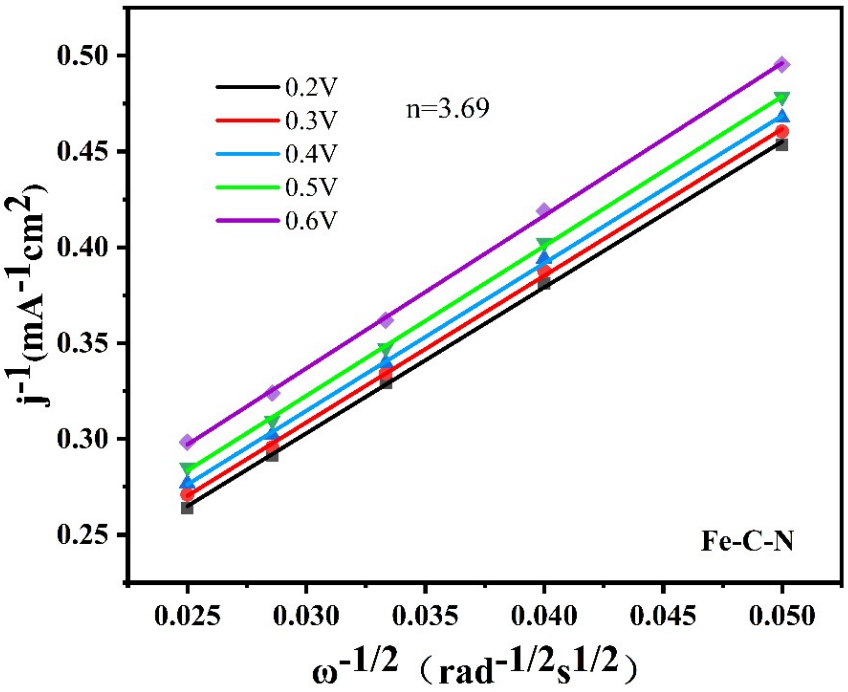

Figure S4. K-L plots of Fe-C-N at different potentials.

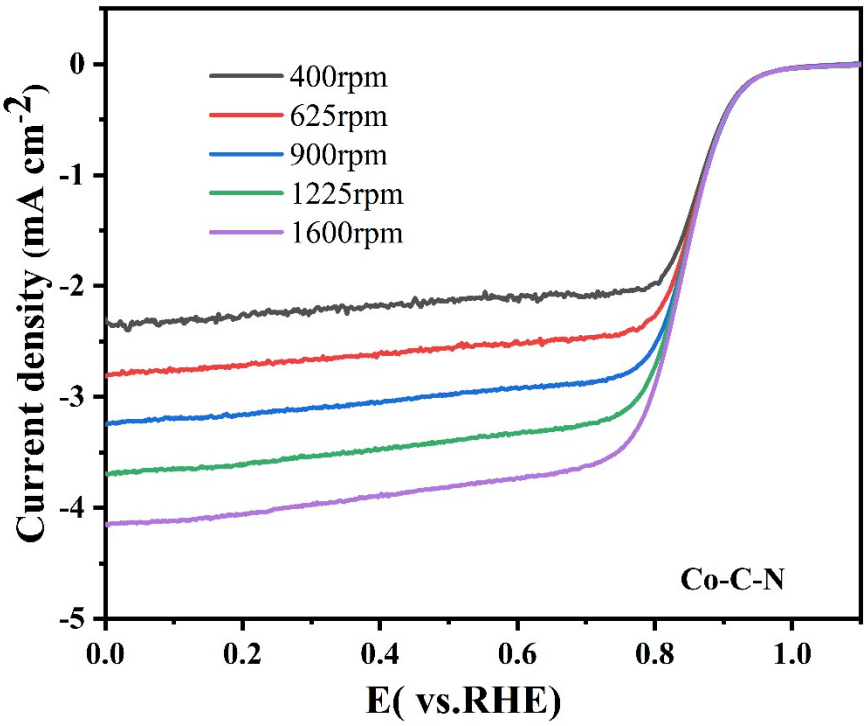

Figure S5. LSV curves of Co-C-N at different rotation speed (400-1600 rpm) in O_2-saturated electrolyte.

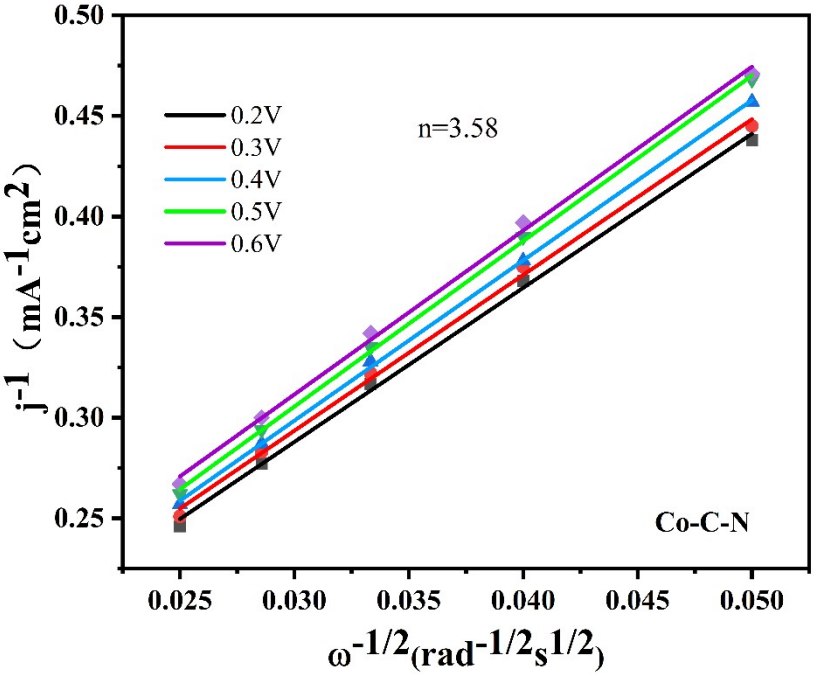

Figure S6. K-L plots of Co-C-N at different potentials.

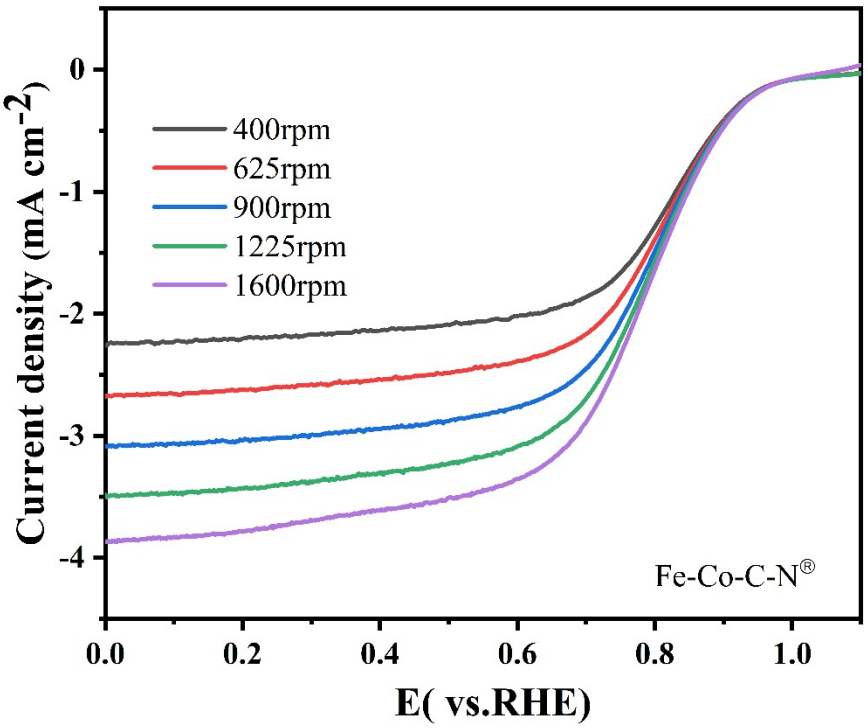

Figure S7. LSV curves of Fe-Co-C-N® at different rotation speed (400-1600 rpm) in O_2-saturated electrolyte.

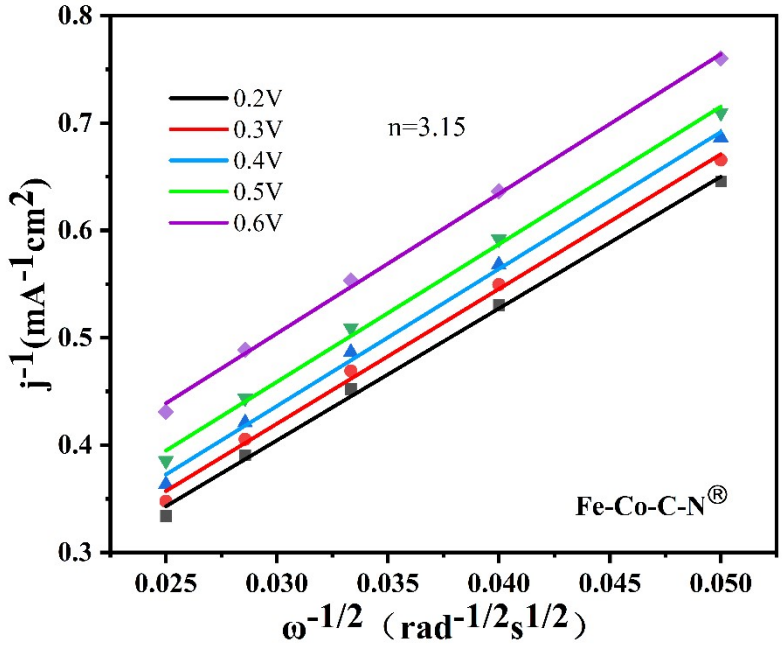

Figure S8. K-L plots of Fe-Co-C-N® at different potentials.

References

1. R. Dun, X. He, J. Huang, W. Wang, l. Yiwei, L. Li, B. Lu, Z. Hua and J. Shi, *Journal of Materials Chemistry A*, 2023, **11**, 5902-5909.
2. S. Juvanen, A. Sarapuu, S. Vlassov, M. Kook, V. Kisand, M. Käärik, A. Treshchalov, J. Aruväli, J. Kozlova, A. Tamm, J. Leis and K. Tammeveski, *ChemElectroChem*, 2021, **8**, 2288-2297.